ENVIRONMENTAL RESEARCH
LETTERS

LETTER • OPEN ACCESS

Extreme sea level variability dominates coastal flood risk changes at decadal time scales

To cite this article: M M Rashid *et al* 2021 *Environ. Res. Lett.* **16** 024026

ENVIRONMENTAL RESEARCH
LETTERS

CrossMark

OPEN ACCESS

RECEIVED
23 October 2020

REVISED
7 December 2020

ACCEPTED FOR PUBLICATION
17 December 2020

PUBLISHED
28 January 2021

LETTER

Extreme sea level variability dominates coastal flood risk changes at decadal time scales

M M Rashid[1], T Wahl[1] and D P Chambers[2]

[1] Civil, Environmental, and Construction Engineering and National Center for Integrated Coastal Research, University of Central Florida, Orlando, FL 32816-2450, United States of America
[2] College of Marine Science, University of South Florida, St. Petersburg, FL, United States of America

E-mail: md.rashid@ucf.edu

Keywords: extreme sea level, coastal flood, annual average losses, amplification factor

Abstract

Coastal flood risk assessments typically ignore interannual to multidecadal variability stemming from mean sea level, storm surges, and long period tides (i.e. 4.4 year perigean and 18.6 year nodal cycles), although combined these can lead to significant variations in extreme sea levels (ESL). Here, we examine the effects of ESL variability on the amplification of flood frequencies and risks for 17 major U.S. coastal cities. We also quantify the relative importance of ESL variability compared to long-term relative sea level rise (RSLR). Results show that, depending on the region, observed ESL variability can lead to amplification factors of up to 79, indicating that the 100 year return period event can become a 1.26 year event during certain time periods when ESL variability peaks high. Additionally, depending on the RSLR scenario considered, the observed range of ESL variability is equivalent to the RSLR projected to occur over the next few years in some locations and several decades (up to 2100) in others. These ESL fluctuations also modulate flood risk estimates, with the aggregated 100 year flood losses for the 17 major U.S. coastal cities changing by up to US$ 141 979 million (or 28%). This study demonstrates the importance of including ESL variability in regional coastal flood risk assessments; it highlights the importance of being aware and vigilant of these variations when observed and projected ESL situations are quantified assuming that certain sea level components are stationary.

1. Introduction

Sea-level rise is the main oceanographic driver for changes in coastal flood risk and it originates from changes and fluctuations of different components such as mean sea level (MSL), storm surges, and long period tides (e.g. Orton *et al* 2016, Vitousek *et al* 2017, Sayol and Marcos 2018, Muis *et al* 2019, Taherkhani *et al* 2020). Higher frequency tides (e.g. diurnal and semidiurnal cycles) can also change over time and lead to increased occurrences of short-term exceedance events, such as high tide flooding (Devlin *et al* 2017, Haigh *et al* 2020, Talke and Jay 2020). However, significant tidal changes usually only occur locally due to anthropogenic impacts, whereas we are interested in variations that are spatially coherent along the coast. Therefore we only include low frequency variability in extreme sea levels due to the 4.4 year perigean and 18.6 year nodal tidal cycles (Haigh *et al* 2011). While interannual to multidecadal variations of these drivers combined may lead to significant changes in extreme sea levels (ESL) (Wahl and Chambers 2015, 2016, Marcos and Woodworth 2017, Rashid *et al* 2019), these are often ignored in coastal flood risk assessments. This can potentially lead to the underestimation of flood risk, leaving coastal infrastructure (at certain times over the anticipated design life) and socio-environmental systems vulnerable. Rashid *et al* (2019) (referred to as R19 hereafter) developed ESL indicators superimposing interannual to multidecadal variability of MSL, storm surge climatology (SSC), and long-period tides for seven regions along the contiguous U.S. coast (figure 1). Regions were separated employing K-means clustering, percent variance explained, and cross correlation so that interannual to multidecadal variability of MSL and SSC of all tide gauges within each region are coherent in terms magnitude and timing. The analysis was carried out separately for the warm season where tropical cyclones occur

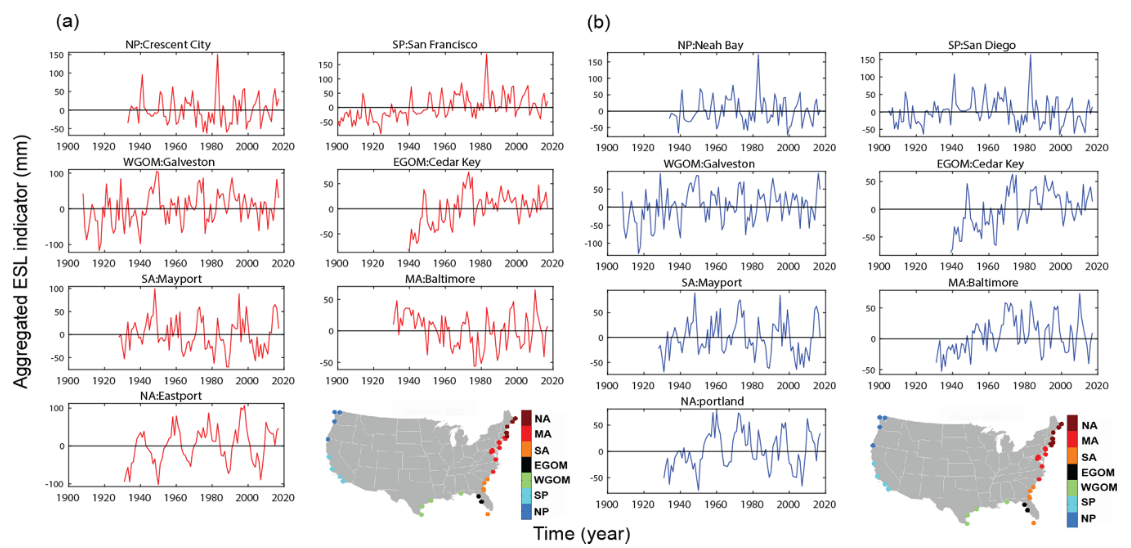

Figure 1. ESL indicators as derived in R19 (and shown as anomalies with mean removed) for regions with coherent ESL variability for summer (a) and winter (b) seasons. Maps represent the spatial domains of coherent regions (NP: U.S. northern Pacific coast, SP: U.S. southern Pacific coast, WGOM: western Gulf of Mexico, EGOM: eastern Gulf of Mexico, SA: South Atlantic, MA: Mid-Atlantic, NA: North Atlantic); for each region R19 identified a representative tide gauge (listed in the panel titles) from where the regional ESL indicators were derived. Results are shown for model A developed in R19 for the storm surge climatology component (see section 2 for details).

more often (summer; May–October) and the cold season where extra-tropical cyclones are more frequent (winter; November–April) to account for storm surge variations from the different storm characteristics. The ESL indicators represent the combination of (a) the interannual variability of MSL after removing the influence of long-term global MSL rise and vertical land motion, (b) the multidecadal variations in SSC expressed as changes in the 100 year return sea levels (similar results exist for all other return periods) after removing the MSL and long period tidal signals, and (c) the fluctuations of the 4.4 year perigean and 18.6 year nodal tidal cycles. Previous studies showed that significant variability exists in both MSL and SSC, and this can often be traced back to large scale climate variations (Dangendorf *et al* 2014, Thompson and Mitchum 2014, Marcos *et al* 2015, Wahl and Chambers 2016, Rashid and Wahl 2020); the role of long period tidal fluctuations in modulating ESL was also explored for some locations, such as the Gulf of Maine (Baranes *et al* 2020). Here we are the first to use the ESL time series displayed in figure 1 to assess the (relative) importance of overall ESL variability (stemming from different components) in modulating extreme event probabilities and coastal flooding risk.

First, we use the concept of amplification factor (Buchanan *et al* 2017, Vitousek *et al* 2017, Oppenheimer *et al* 2019, Frederikse *et al* 2020) to quantify how the occurrence frequency of a certain extreme event (here the 100 year return sea level) changed in the past due to observed ESL variability alone. Second, we explore the relative importance of ESL variability by quantifying the expected time scales in the future when RSLR would increase by an amount equivalent to the range of ESL variability. We also repeat the analysis for the three components of ESL (i.e. MSL, SSC, and long period tides) separately to identify the contributions of each component. Finally, we assess how ESL variability can modulate flood risk when compared to the stationarity assumption (i.e. ignoring ESL variability). For this purpose we employ the model introduced by Hallegatte *et al* (2013) (referred to as H13 hereafter) and focus on 100 year flood exposure and economic losses for 17 U.S. major coastal cities with populations larger than one million (in 2005).

2. Data and methods

In R19 a nonstationary generalized extreme value (GEV) model was fitted to seasonal (summer and winter) water level maxima to quantify SSC variability. Hourly sea level data of tide gauges along the contiguous U.S. coastline were used. SSC variability was quantified as the nonstationary 100 year sea level after removing the effects of MSL and long-period tides, hence representing the decadal to multidecadal variability of SSC. Two approaches were adopted: one considers that only the location parameter of the GEV distribution varies with time (referred to as model A) and the other one considers that both the location and scale parameters of the GEV distribution are time varying (referred to as model B), while the shape parameter is assumed constant for both cases. MSL variability represents the interannual fluctuations of MSL after removing the influence of global MSL rise and vertical land motion. The SSC variability derived with the two models was then combined with the MSL variability and long period tidal fluctuations

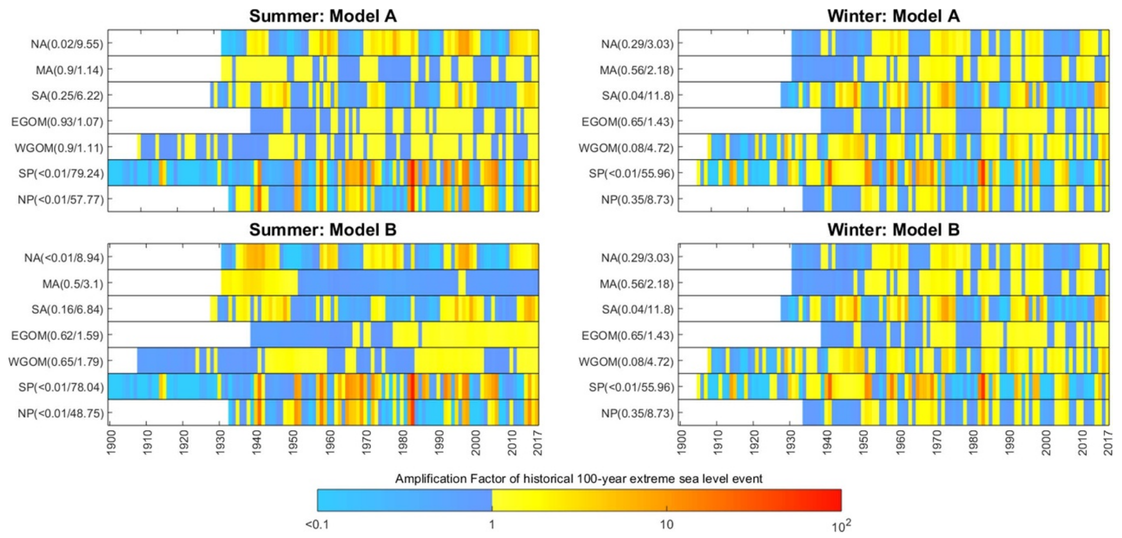

Figure 2. Amplification factors (color map) of present-day stationary 100 year sea levels due to observed ESL variability from 1900 to 2017 for regions with coherent ESL variability along the U.S. coastline; results are shown for different seasons (summer and winter) and models to quantify SSC variability (models A and B). Numbers in brackets denote minimum and maximum amplification factors. NP: U.S. northern Pacific coast, SP: U.S. southern Pacific coast, WGOM: western Gulf of Mexico, EGOM: eastern Gulf of Mexico, SA: South Atlantic, MA: Mid-Atlantic, NA: North Atlantic.

to derive the ESL indicators. Figure 1 shows results for model A where the range of variability reaches approximately 10–20 cm; for model B (not shown, see R19 for details) variability is even larger and also considered here to assess the importance of ESL variability (Washid *et al* 2019).

As mentioned in the introduction, we first explore how ESL variability modulated the probability of a certain extreme event in the past. We employ the concept of amplification factor using the same distributional based frequency transfer method as in earlier studies (e.g. Vitousek *et al* 2017, Oppenheimer *et al* 2019). The amplification factor indicates the change of the average occurrence probability of a certain extreme event (here we chose the 100 year return sea level). Therefore, an amplification factor of 100 indicates, for example, that the sea level corresponding to a 100 year return period becomes an annual event. Amplification factors larger (lower) than 1 indicate that the occurrence frequency of the selected extreme event increased (decreased), whereas 1 indicates no change. Typically, amplification factors are derived for future RSLR scenarios, but here we quantify in a first step the amplification factors due to past sea level changes associated only with ESL variability. We carry out the analysis separately for the summer and winter seasons and by using the GEV distribution parameters from models A and B in R19.

In the next step we explore the relative importance of ESL variability compared to the projected RSLR derived by Sweet *et al* (2017) for the U.S. tide gauges; these sea level scenarios include estimates of vertical land motion from (Zervas *et al* 2013) which are projected into the future. We consider the local RSLR for the representative tide gauges where the ESL indicators were defined; we use the intermediate-low (global mean 0.5 m), intermediate-high (global mean 1.5 m), and extreme (global mean 2.5 m) scenarios, respectively. We quantify the observed range (i.e. maximum minus minimum) of ESL variability for each region and estimate when RSLR is expected to increase by an amount equivalent to the range of ESL variability. Since the ESL indicators are formulated from three components (i.e. interannual MSL variability, multidecadal SSC variability, and long period tidal fluctuations) we repeat the analysis but considering the range of each individual component.

Finally, we adopt the H13 model to quantify how ESL variability modulates flood exposure and economic losses for 17 major coastal cities. The H13 model uses a stationary extreme value distribution and estimates flood losses for 136 coastal cities (each with more than 1 million inhabitants in 2005) globally, of which 17 are in the U.S. The model combines ESL and future sea-level rise information with land subsidence, elevation, population, and gross domestic product data for present-day and under future socio-economic scenarios (including coastal adaptation) to quantify flood risk at the city level. In order to assess the role of ESL variability in modulating flood risk, we modify the ESL distributions for the 17 cities by adding the identified range of ESL variability from the corresponding region. ESL fluctuates around the center (figure 1) with high or low peaks which cause increase or decrease in flood risk. Ranges from the center to the highest and lowest peaks are considered for analyzing corresponding increase and decrease in flood risk. The ranges of ESL variability are different for summer and winter seasons and for each city we consider the one with the higher range to

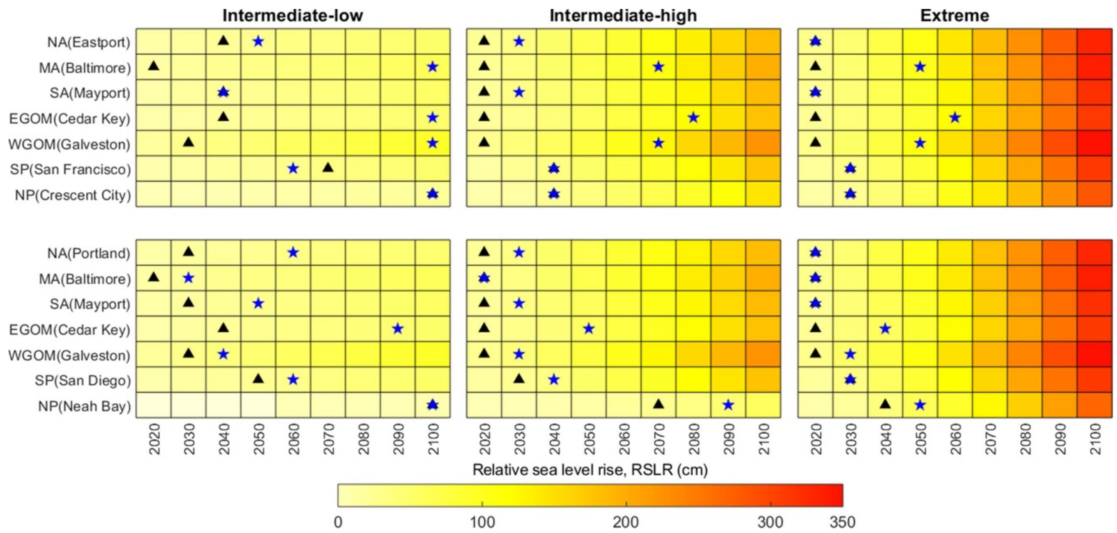

Figure 3. RSLR (color map) at representative tide gauges corresponding to regions of coherent ESL variability for three different RSLR scenarios. Markers represent the time scales when RSLR is expected to reach an amount equivalent to the range of ESL variability for model A (triangle) and model B (star) for the summer (top row) and winter (bottom row) seasons; note that RSLR is identical for the same tide gauge in both seasons.

capture the full spectrum of observed ESL variability. Then we estimate exposure and losses of the 100 year flood event with the original and modified ESL distributions and compare the results to quantify how ESL variability can modify flood risk, assuming present-day (here 2005) socio-economic conditions. Since we focus on present day, we do not include scenarios of sea-level rise, subsidence, and future socio-economic development.

3. Results

Figure 2 shows the amplification factors for the different regions with coherent ESL variability for different seasons (summer and winter) and different models used to quantify the SSC variability (models A and B). There were periods in the 20th and early 21st centuries where ESL variability alone (RSLR is not included) caused amplification factors between 10 and 100, indicating that the 100 year event (under the stationarity assumption) was a 1 to 10 year event and hence more likely to occur during different time periods in the past. It is also expected that similar changes occur in the future due to continuing ESL variability. Amplification factors vary across regions, seasons, and models. Larger amplification factors are found for the regions along the U.S. Pacific coast compared to the Gulf and east coasts for both models (models A and B) and seasons. The highest amplification factors for the U.S. north Pacific and south Pacific regions were 79.2 and 57.8, respectively. For other regions amplification factors vary within a range of 1.1–11.8. Note that the amplification factors are not only impacted by the range of ESL variability, but also the scale and shape parameters of the extreme value distribution in the respective region. Regions with heavy tailed (shape parameter > 0) extreme value distributions due to large storm surge events show relatively lower amplification factors compared to the regions with thin tailed distributions (shape parameter < 0). There were also periods when amplification factors were <1 indicating that the stationary 100 year water level was less likely to be exceeded and turned into the 500 year or 1000 year event. While the magnitudes of these highs and lows of ESL are crucial in terms of coastal planning and management, the exact times when they occur are challenging to predict. This was shown, for example, in Rashid and Wahl (2020), who explored the applicability of statistical downscaling with initialized decadal climate model simulations for this purpose. Additionally, non-oceanographic drivers such as river discharge directly or indirectly (through nonlinear interactions with oceanographic drivers) may contribute to ESL variability leading to amplification of extremes, particularly in the fresh-water influenced coastal regions (Buschman *et al* 2009, Hoitink and Jay 2016). However, such effects are more local, while our focus is on the spatially coherent variability that can be traced back to large-scale climate variations.

Next, we extend the analysis from historical to future periods, by comparing the historical ESL variability to future RSLR for the representative tide gauges of the different regions with coherent variability (y-axis tick labels in figure 3). While any tide gauge in a region could be used to derive the local RSLR, we consider the representative tide gauges identified in R19 for consistency. We explore the relative importance of ESL variability compared to future RSLR (color map in figure 3) by translating the range of observed ESL variability into time scales when the equivalent amount of RSLR is expected to

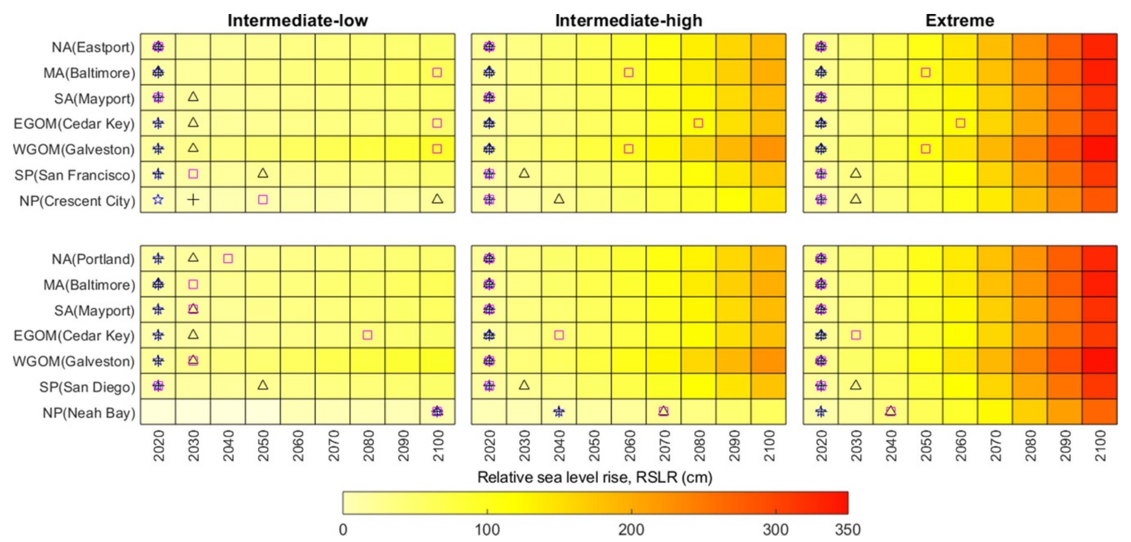

Figure 4. RSLR (color map) at representative tide gauges corresponding to different regions with coherent ESL variability for three different RSLR scenarios. Markers represent the time scales when RSLR is expected to reach the amount equivalent to the range of observed variability of long period tides (star), MSL (triangle), SSC from model A (plus), and SSC from model B (square) for the summer (top row) and winter (bottom row) seasons; note that RSLR is identical for the same tide gauge in both seasons.

occur (markers in figure 3). The results highlight that, depending on the region and RSLR scenario considered, the amount of ESL variability is equivalent to RSLR that is expected to occur over time scales varying from a few years up to several decades into the future (in some instances 2100). As expected, the time scales are longer for model B compared to model A, because the estimated SSC variability is relatively larger for model B.

In order to assess the relative importance of the three components which contribute to the overall ESL variability, we repeat the same analysis but separately to estimate when RSLR reaches the equivalent amount of variability stemming from long period tides, MSL, and SSC (figure 4). Results show that the variability of long period tides are equivalent to RSLR that is expected to occur in the 2020s because their variability is relatively smaller. In contrast, MSL and SSC variability are more dominant having relatively larger ranges of variability. Depending on the region and scenario, MSL variability is equivalent to the amount of RSLR that is expected to occur in the 2030s to 2050s, whereas SSC variability in some instances is equivalent to the amounts of RSLR which are expected in the 2050s to 2080s (under the intermediate-high and extreme rise scenarios) or even by 2100 (under the intermediate-low sea-level rise scenario).

Results discussed so far show that there are periods ranging from years to decades in the historical records where ESL were relatively higher or lower than normal, and that this ESL variability is equivalent to the RSLR projected to occur in the next few years up to the end of the 21st century in some instances. This reveals that ESL variability is also a prominent driver modulating coastal flood risks during certain time periods. To assess this further, we employ the H13 model to estimate flood exposure and losses for 17 major U.S. coastal cities, considering ESL variability in addition to the stationary ESL used in the original study by Hallegatte *et al* (2013). High and low peaks of ESL fluctuate around the center (figure 1) causing increase and decrease in flood risk during certain time periods.

Table 1 exhibits how ESL variability translates to changes in 100 year flood exposure and losses (in million dollars), highlighting significant changes for all cities considered here, and, as before, with stronger effects when model B is used to derive the SSC variability component. In general, cities along the U.S. east and Gulf coasts show larger changes in flood losses (in terms of absolute values), compared to the U.S. west coast. However, relative changes in flood losses due to ESL variability for the cities along the U.S. west coast are also prominent when compared to the exposure and losses found in H13 (percentage values are shown in parentheses in table 1). The regional variability of changes in flood exposure and losses derived here, not only depends on the range of ESL variability, but also differences in topographic gradients, and spatial distribution of exposed populations and assets. Aggregated losses (of the 100 year flood event) from the 17 selected U.S. coastal cities increase up to approximately US$ 14 386 million (model A) and US$ 67 535 million (model B) due to high peaks of ESL, which represents relative changes of 3% and 13%. On the other hand, low peaks of ESL reduce the aggregated flood losses up to approximately US$ 21 253 (model A) and US$ 74 444 (model B), which represents relative changes of 4% and 14%. This reveals that the total modulation of flood risk due to the full range of ESL variability (from lowest peak to highest peak) in terms of 100 year flood losses are

Table 1. Present-day (2005) flood risk (100 year event exposure and losses without protection) for 17 U.S. major coastal cities assuming stationary ESL and their modulations (increase or decrease) due to ESL variability (high and low peaks).

		Flood risk under assumed stationary ESL (H13) (US$ million)		Modulation of flood risk due to ESL variability (US$ million)							
				Increase in flood risk due to high peak in ESL variability				Decrease in flood risk due low peak in ESL variability			
				Model A		Model B		Model A		Model B	
Regions	Major U.S. coastal cities	100 year exposure	100 year losses	100 year exposure	100 year losses	100 year exposure	100 year losses	100 year exposure	100 year losses	100 year exposure	100 year losses
NP	Seattle	4549	2711	82 (2%)	67 (2%)	160 (4%)	131 (5%)	−113 (−2%)	−104 (−4%)	−156 (−3%)	−139 (−5%)
	Portland	1668	763	45 (3%)	49 (6%)	67 (4%)	72 (9%)	−45 (−3%)	−52 (−7%)	−45 (−3%)	−52 (−7%)
	San Francisco—Oakland	15 180	5885	1411 (9%)	726 (12%)	1411 (9%)	726 (12%)	−2121 (−14%)	−1034 (−18%)	−2121 (−14%)	−1034 (−18%)
SP	San Jose	1256	414	215 (17%)	107 (26%)	215 (17%)	107 (26%)	−201 (−16%)	−100 (−24%)	−201 (−16%)	−100 (−24%)
	Los Angeles—Long Beach	15 926	6896	654 (4%)	571 (8%)	654 (4%)	571 (8%)	−1239 (−8%)	−882 (−13%)	−1239 (−8%)	−882 (−13%)
	San Diego	609	325	35 (6%)	17 (5%)	35 (6%)	17 (5%)	−26 (−4%)	−17 (−5%)	−26 (−4%)	−17 (−5%)
WGOM	Houston	12 954	5483	539 (4%)	480 (9%)	3184 (25%)	2401 (44%)	−774 (−6%)	−487 (−9%)	−4076 (−31%)	−2356 (−43%)
	New Orleans	143 963	80 287	1165 (1%)	1694 (2%)	5121 (4%)	8277 (10%)	−1381 (−1%)	−1837 (−2%)	−8229 (−6%)	−12 208 (−15%)
EGOM	Tampa—St Petersburg	49 593	24 958	704 (1%)	564 (2%)	16 519 (33%)	7943 (32%)	−1565 (−3%)	−1143 (−5%)	−8374 (−17%)	−6576 (−26%)
SA	Miami	366 421	172 160	5822 (2%)	4939 (3%)	16 851 (5%)	9896 (6%)	−12 939 (−4%)	−10 202 (−6%)	−19 408 (−5%)	−15 465 (−9%)
	Baltimore	14 042	6847	151 (1%)	155 (2%)	2072 (15%)	1402 (20%)	−167 (−1%)	−161 (−2%)	−1522 (−11%)	−1682 (−25%)
	Washington, DC	5478	2654	141 (3%)	74 (3%)	1252 (23%)	634 (24%)	−243 (−4%)	−144 (−5%)	−1012 (−18%)	−633 (−24%)
MA	Virginia Beach	61 507	27 854	2290 (4%)	1288 (5%)	15 892 (26%)	11 328 (41%)	−2544 (−4%)	−1222 (−4%)	−23 150 (−38%)	−8645 (−31%)
	Philadelphia	22 132	12 192	257 (1%)	203 (2%)	2412 (11%)	1599 (13%)	−513 (−2%)	−412 (−3%)	−2328 (−11%)	−1959 (−16%)
	New York—Newark	236 530	129 657	3088 (1%)	2234 (2%)	34 159 (14%)	20 680 (16%)	−3088 (−1%)	−2264 (−2%)	−28 066 (−12%)	−21 417 (−17%)
NA	Providence	7936	4213	236 (3%)	174 (4%)	236 (3%)	174 (4%)	−232 (−3%)	−175 (−4%)	−354 (−4%)	−262 (−6%)
	Boston	55 445	30 966	1659 (3%)	1045 (3%)	2488 (4%)	1578 (5%)	−1659 (−3%)	−1018 (−3%)	−1659 (−3%)	−1018 (−3%)
Total		1 015 191	514 266	18 494 (2%)	14 386 (3%)	102 727 (10%)	67 535 (13%)	−28 852 (−3%)	−21 253 (−4%)	−101 966 (−10%)	−74 444 (−14%)

Percentage values within parentheses represent relative changes compared to H13.

approximately US$ 35 639 (14 386 + 21 253) million for model A and US$ 141 979 million for model B, which are equivalent to 7% and 28% of losses found in H13.

4. Conclusions

In this study we explore how ESL variability from the combination of interannual to multidecadal variability of long period tides, MSL, and SSC can modulate flood risk. First, we quantify amplification factors of the present-day 100 year ESL event over the historic period. We identify periods (years to decades) in the 20th and 21st centuries where amplification factors ranged from <0.01 (i.e. it was less likely that the present-day 100 year ESL was exceeded) to >50 (i.e. the 100 year ESL had a return period of less than 2 years). The largest amplification factors were found for the U.S. north Pacific and south Pacific regions, with values of 79.2 and 57.8, respectively, indicating that the 100 year events were 1.26 year and 1.73 year events. We expect similar ESL variability to continue to occur in the future along with RSLR and we compare the relative importance of the two. Depending on the region, RSLR scenario, and extreme value model used for SSC analysis (models A or B), the range of ESL variability is equivalent to RSLR expected to occur in the next few years up to several decades (for few cases as late as 2100). Finally, we assess the role of ESL variability in modulating coastal flood risk by employing the H13 model. We quantify how ESL variability alone can change 100 year flood exposure and losses for 17 major U.S. coastal cities. Aggregated flood losses across all 17 cities can be modulated (from low to high peak of ESL variability) by approximately US$ 356 639 million (for model A) and US$ 141 979 million (for model B), or 7% and 28%, respectively. This study reveals the important role of ESL variability in amplifying the occurrence frequency of critical ESL events and for modulating flood exposure and losses in addition to RSLR at interannual to multidecadal timescales. It is therefore crucial to be aware of and account for ESL variability in flood risk assessments, infrastructure design, and decision-making.

Data availability statement

The data that support the findings of this study are openly available at the following URL/DOI: https://doi.org/10.6084/m9.figshare.9782297.v2.

Acknowledgments

We acknowledge the National Oceanic and Atmospheric Administration (NOAA), University of Hawaii Sea Level Center (UHSLC), Global Extreme Sea Level Analysis (GESLA) database for and Permanent Service for Mean Sea Level (PSMSL) for providing hourly and monthly sea level data. This study was supported by NOAA's Climate Program Office, Climate Monitoring Program, Award Number NA17OAR4310158

ORCID iDs

M M Rashid https://orcid.org/0000-0002-0315-9055
T Wahl https://orcid.org/0000-0003-3643-5463

References

Baranes H, Woodruff J, Talke S, Kopp R, Ray R and Deconto R 2020 Tidally driven interannual variation in extreme sea level frequencies in the Gulf of Maine *J. Geophys. Res. Oceans* **125** e2020JC016291

Buchanan M K, Oppenheimer M and Kopp R E 2017 Amplification of flood frequencies with local sea level rise and emerging flood regimes *Environ. Res. Lett.* **12** 064009

Buschman F, Hoitink A, Van Der Vegt M and Hoekstra P 2009 Subtidal water level variation controlled by river flow and tides *Water Resour. Res.* **45** W10420

Dangendorf S, Calafat F M, Arns A, Wahl T, Haigh I D and Jensen J 2014 Mean sea level variability in the North Sea: processes and implications *J. Geophys. Res. Oceans* **119** 6820–41

Devlin A T, Jay D A, Zaron E D, Talke S A, Pan J and Lin H 2017 Tidal variability related to sea level variability in the Pacific Ocean *J. Geophys. Res. Oceans* **122** 8445–63

Frederikse T, Buchanan M K, Lambert E, Kopp R E, Oppenheimer M, Rasmussen D and van de Wal R S 2020 Antarctic ice sheet and emission scenario controls on 21st-century extreme sea-level changes *Nat. Commun.* **11** 1–11

Haigh I D, Eliot M and Pattiaratchi C 2011 Global influences of the 18.61 year nodal cycle and 8.85 year cycle of lunar perigee on high tidal levels *J. Geophys. Res. Oceans* **116** C06025

Haigh I D, Pickering M D, Green J M, Arbic B K, Arns A, Dangendorf S, Hill D F, Horsburgh K, Howard T and Idier D 2020 The tides they are a-changin': a comprehensive review of past and future nonastronomical changes in tides, their driving mechanisms, and future implications *Rev. Geophys.* **58** e2018RG000636

Hallegatte S, Green C, Nicholls R J and Corfee-Morlot J 2013 Future flood losses in major coastal cities *Nat. Clim. Change* **3** 802

Hoitink A and Jay D A 2016 Tidal river dynamics: implications for deltas *Rev. Geophys.* **54** 240–72

Marcos M, Calafat F M, Berihuete Á and Dangendorf S 2015 Long-term variations in global sea level extremes *J. Geophys. Res. Oceans* **120** 8115–34

Marcos M and Woodworth P L 2017 Spatiotemporal changes in extreme sea levels along the coasts of the North Atlantic and the Gulf of Mexico *J. Geophys. Res. Oceans* **122** 7031–48

Muis S, Lin N, Verlaan M, Winsemius H C, Ward P J and Aerts J C 2019 Spatiotemporal patterns of extreme sea levels along the western North-Atlantic coasts *Sci. Rep.* **9** 1–12

Oppenheimer M, Glavovic B, Hinkel J, van de Wal R, Magnan A K, Abd-Elgawad A, Cai R, Cifuentes-Jara M, Deconto R M and Ghosh T 2019 Sea level rise and implications for low lying islands, coasts and communities

Orton P M, Hall T, Talke S A, Blumberg A F, Georgas N and Vinogradov S 2016 A validated tropical-extratropical flood hazard assessment for New York Harbor *J. Geophys. Res. Oceans* **121** 8904–29

Rashid M M, Wahl T, Chambers D P, Calafat F M and Sweet W V 2019 An extreme sea level indicator for the contiguous United States coastline *Sci. Data* **6** 1–14

Rashid M and Wahl T 2020 Predictability of extreme sea level variations along the US coastline *J. Geophys. Res. Oceans* **125** e2020JC016295

Sayol J and Marcos M 2018 Assessing flood risk under sea level rise and extreme sea levels scenarios: application to the ebro delta (Spain) *J. Geophys. Res. Oceans* **123** 794–811

Sweet W V, Kopp R E, Weaver C P, Obeysekera J, Horton R M and Thieler E R 2017 Global and regional sea level rise scenarios for the United States *NOAA Tech. Rep.* NOS CO-OPS 83

Taherkhani M, Vitousek S, Barnard P L, Frazer N, Anderson T R and Fletcher C H 2020 Sea-level rise exponentially increases coastal flood frequency *Sci. Rep.* **10** 1–17

Talke S A and Jay D A 2020 Changing tides: the role of natural and anthropogenic factors *Ann. Rev. Mar. Sci.* **12** 121–51

Thompson P and Mitchum G 2014 Coherent sea level variability on the North Atlantic western boundary *J. Geophys. Res. Oceans* **119** 5676–89

Vitousek S, Barnard P L, Fletcher C H, Frazer N, Erikson L and Storlazzi C D 2017 Doubling of coastal flooding frequency within decades due to sea-level rise *Sci. Rep.* **7** 1–9

W Rashid M M, Wahl T, Chamber D P, Calafat F M and Sweet W V 2019 Database for extreme sea level indicators for the contiguous United States coastline (https://doi.org/10.6084/m9.figshare.9782297.v2)

Wahl T and Chambers D P 2015 Evidence for multidecadal variability in US extreme sea level records *J. Geophys. Res. Oceans* **120** 1527–44

Wahl T and Chambers D P 2016 Climate controls multidecadal variability in US extreme sea level records *J. Geophys. Res. Oceans* **121** 1274–90

Zervas C, Gill S and Sweet W 2013 Estimating vertical land motion from long-term tide gauge records *Technical Report* NOS CO-OPS 065 (Silver Spring, MD: NOAA)